Performance Analysis of UWB Systems in the Presence of Timing Jitter

İsmail Güvenç and Hüseyin Arslan

Abstract: In this paper, performances of different ultra-wideband (UWB) modulation schemes in the presence of timing jitter are evaluated and compared. Static and Rayleigh fading channels are considered. For fading channels, flat and dispersive channels are assumed. First, bit error rate (BER) performances for each case are derived for a fixed value of timing jitter. Later, a uniform distribution of jitter is assumed to evaluate the performance of the system, and the theoretical results are verified by computer simulations. Finger estimation error is treated as timing jitter and an appropriate model is generated. Furthermore, a worst case distribution that provides an upper bound on the system performance is presented and compared with other distributions. Effects of timing jitter on systems employing different pulse shapes are analyzed to show the dependency of UWB performance on pulse shape. Although our analysis assumes uniform timing jitter, our framework can be used to evaluate the BER performance for any given probability distribution function of the jitter.

Index Terms: Maximal ratio combining, multiband UWB, performance analysis, Rake receivers, timing jitter, ultra-wideband.

I. INTRODUCTION

Although the idea was known long ago, ultra-wideband (UWB) technology has recently become popular after the release of Federal Communications Commission's (FCC) Part 15 Rules. These rules allow UWB devices to operate between 3.1 and 10.6 GHz with transmission power levels up to -41 dBm/MHz. UWB is an attractive technology since it is capable of offering very high data rates achieved by the transmission of short duration pulses. UWB transceivers are low cost and simple compared with the other narrowband transceivers. UWB systems operate at very low power levels due to their high fractional bandwidths[1], causing very low interference to other technologies. Since its bandwidth is much larger than the coherence bandwidth of the channel and any deep fades effect only a small portion of the total bandwidth, robustness against channel fading is obtained without the need for multiple antenna transceivers. Its usage for positioning technologies with a potential of sub-decimeter accuracy; its suitability for wireless sensor networks due to its simple, low-cost, low-power transceiver circuitry; robustness to eavesdropping due to used time-hopping pseudo-noise (TH-PN) sequences; and easier material penetration because of the wide frequency range are some other advan-

tages to note.

Due to extremely short duration of pulses used, UWB systems require high sensitivity against timing errors for proper demodulation of the received signal. Ideally, transmitted pulses in a digital communication system arrive at the receiver at integer multiples of sampling times. In real systems, pulses are received at times that are different from integer multiples of sampling times, which is named as timing jitter [1]. The traditional way to measure the timing jitter is using the *eye pattern* observed in an oscilloscope, which is the synchronized and superimposed possible realizations of the received signal viewed within a particular signaling interval [2]. The thickness of the eye edges gives an idea about the range of the timing jitter.

According to the sources of timing jitter, it can be examined in two categories: Random jitter and deterministic jitter [3]–[5]. Random jitter is assumed to be Gaussian in nature, and is caused by the accumulation of thermal noise sources [5]. Generally, deterministic jitter is bounded and non-Gaussian. Some examples for deterministic jitter are duty-cycle distortion, e.g., from asymmetric rise/fall times; inter-symbol interference, e.g., from channel dispersion or filtering; sinusoidal, e.g., from power supply feed-through; and uncorrelated, e.g., crosstalk by other signals [5]. The total jitter thus can have both random and deterministic components, and its PDF can be obtained by the convolution of the PDFs of the random jitter and the deterministic jitter [4]. Deterministic jitter can be reduced or eliminated once its source is determined [3]. Using the eye pattern technique, or the histogram technique in an oscilloscope, it is possible to distinguish between the random and deterministic components of the total jitter.

Effects of timing jitter on the performances of different technologies have been investigated in the past [6]–[8], and various methods are proposed to model the jitter distribution [4], [9]–[11]. Effect of timing jitter on the signal power spectral density (PSD) in a multipath environment has been analyzed in [12]. Surveys and books have been written to clarify the relationships between different jitter aspects and measurement techniques [1], [13], [14].

New UWB radios are capable of precisely positioning the sub-nanosecond pulses with a Gaussian distributed root-mean-squared (RMS) jitter of 10 ps and within a 50 ns time window [15]. Even if the transceiver clocks are very stable and introduce very little jitter, other issues such as timing tracking and relative velocities between transmitter and receiver introduce additional degradation in synchronization [16].

Although timing jitter has a significant effect on the BER performance of UWB systems, theoretical performance analyses for UWB systems in the presence of timing jitter have not been done to the best knowledge of the authors. Especially, accurate

[1]Fractional bandwidth is defined as the ratio of the system's bandwidth to central frequency. For a UWB system, either the fractional bandwidth has to be larger than 20%, or the system bandwidth has to be larger than 500 MHz.

mathematical modeling and theoretical BER analysis of the effect of timing jitter is required. Performance analysis of UWB modulation schemes in ideal conditions [17] and in other practical scenarios such as multipath [18], multiple access interference [19] and narrowband interference [20] have been done in the past. The effect of timing jitter on the PSD of UWB signals has been analyzed in [21]–[23] and it was concluded that jitter in fact helped to *smooth* the PSD due to the introduced randomness. The effect of uniformly distributed timing jitter on the UWB performance were simulated in [24] for optimum pulse position modulation (PPM) and in [25] for Hermite polynomial pulses. Lovelace *et al.* analyze the performance degradation in the multiple access capability of the UWB system in the presence of Gaussian distributed timing jitter for binary and M-ary PPM schemes [16].

The focus of this paper is the theoretical performance anaysis of UWB systems in the presence of timing jitter. The effects of timing jitter on the performances of orthogonal-PPM, optimum-PPM, on-off keying (OOK), and binary phase shift keying (BPSK) modulations are investigated. Theoretical BER equations for static and Rayleigh fading channels in the presence of timing jitter are derived and compared with simulations. For Rayleigh fading channels, flat and dispersive channel models are used. Based on [6], a worst case jitter distribution that can serve as an upper bound on the system performance is presented, and the effect of the pulse shape is analyzed.

The paper is organized as follows. Section II gives a generic UWB system model for PPM and BPSK modulations. BER formulations under timing jitter are presented and compared with simulations in Section III. In Section IV, the effect of timing jitter PDF on system performance is analyzed, and the PDF for jitter due to finger estimation error is presented. Section V analyzes the effect of pulse shape on system performance when there is jitter, and the last section concludes the paper.

II. SYSTEM MODEL

A. Signal Model

For UWB systems, generic transmitted signal $s^{(k)}(t)$ and received signal $r^{(k)}(t)$ by desired user ($k = 1$) in a single-path, and multi-user environment can be written as

$$s^{(1)}(t) = \sum_{n=-\infty}^{\infty} \sum_{j=0}^{N_s-1} \sqrt{A}\beta^{(1)}(n)\omega_{tr}(t - (nN_s + j)T_f - c_j^{(1)}T_h - \delta\alpha^{(1)}(n)), \tag{1}$$

$$r^{(1)}(t) = \sum_{k=1}^{N_u} \sum_{n=-\infty}^{\infty} \sum_{j=0}^{N_s-1} \sqrt{A}\beta^{(k)}(n)\omega_{rx}(t - (nN_s + j)T_f - c_j^{(k)}T_h - \delta\alpha^{(k)}(n) + \tilde{\tau}^{(k)} - \epsilon_j(n)) + \tilde{n}(t), \tag{2}$$

where k, n, and j are the user, bit, and frame numbers, respectively, T_f is the nominal interval between two pulses, N_s is the number of pulses per symbol, and δ is the modulation index if the modulation is PPM. T_h is the chip duration which is equal to pulse width T_c for antipodal modulation schemes and δ larger than T_c for PPM. Decimal codes $\{c_j^{(k)}\}$ are pseudo-random

codes unique to user k, and are used to implement time hopping (TH) UWB as the multiple access scheme. The timing jitter for the jth pulse, ϵ_j, is a zero-mean random variable, and $\tilde{\tau}^{(k)}$ is the delay of each user in an asynchronous system. Pulse amplitude is represented by $\sqrt{A}$, and $\tilde{n}(t)$ is the additive white Gaussian noise (AWGN) with double-sided spectrum of $\frac{N_0}{2}$. With $\beta^{(k)}(n)$ changing the amplitudes of the pulses (OOK, BPSK) or $\delta\alpha^{(k)}(n)$ varying the time positions of the pulses (PPM), UWB signals can be modulated in different ways as shown in Table 1.

The transmitted *mono-cycle* is represented by ω_{tr}. Due to the differentiation effects of the antennas, received pulse ω_{rx} is modeled as the derivative of the *mono-cycle*

$$\omega_{rx}(t) = [1 - 4\pi(\frac{t}{\tau})^2]e^{-2\pi(\frac{t}{\tau})^2}, \tag{3}$$

where τ is directly proportional with the pulse width, T_c. The autocorrelation function of the received pulse, the energy of the received pulse, and the total energy per bit are respectively expressed as

$$R(\Delta t) = \frac{\int_{-\infty}^{\infty} \omega_{rx}(t)\omega_{rx}(t - \Delta t)dt}{\int_{-\infty}^{\infty} \omega_{rx}^2(t)}$$

$$= \left[1 - 4\pi(\frac{\Delta t}{\tau})^2 + \frac{4\pi^2}{3}(\frac{\Delta t}{\tau})^4\right]e^{-\pi(\frac{\Delta t}{\tau})^2}, \tag{4}$$

$$E_p = \int_{-\infty}^{\infty} \omega_{rx}^2(t)dt, \tag{5}$$

$$E_b = N_s A E_p. \tag{6}$$

At the receiver, the received signal is correlated with a template and a decision is made based on the detection algorithm. The correlator template used for PPM is given by

$$v(t) = \omega_{rx}(t) - \omega_{rx}(t - \delta). \tag{7}$$

Note that δ is larger than T_c for orthogonal PPM and smaller than T_c for overlapped PPM. Optimum PPM is achieved by selecting δ that minimizes $R(\delta)$, or maximizes $1 - R(\delta)$. For BPSK and OOK, ω_{rx} itself is used as the template. Templates used for BPSK and optimum PPM, and the received pulse with jitter when transmitting *zero* are depicted in Fig. 1.

Output of the correlator is found by multiplying and integrating the received pulse with the receiver template

$$U = \int_{-\infty}^{\infty} r^{(1)}(t)v(t)dt. \tag{8}$$

This value can then be used to make a binary decision for BPSK and PPM as follows

$$b = \begin{cases} 0, & \text{if } U \geq 0 \\ 1, & \text{if } U < 0 \end{cases}, \tag{9}$$

where b denotes the detected bit. For OOK, U is compared with a threshold T to make a decision

$$b = \begin{cases} 0, & \text{if } U \leq T \\ 1, & \text{if } U > T \end{cases}. \tag{10}$$

Normalized correlation functions of the received pulse with the templates used in BPSK and optimum PPM schemes are depicted in Fig. 2. Notice that correlation functions, and therefore

Table 1. UWB modulation options and BER performances.

Modulation Scheme	$\beta^{(k)}(n)$	$\delta\alpha^{(k)}(n)$	BER
Orthogonal PPM	1	$0, T_c$	$Q\left(\sqrt{\frac{N_s A E_p}{N_0}}\right)$
Optimum PPM	1	$0, \delta_{opt},$ $\delta_{opt} = \arg\max_{\delta}\{1 - R(\delta)\}$	$Q\left(\sqrt{\frac{N_s A E_p}{N_0}(1 - R(\delta_{opt}))}\right)$
BPSK	± 1	0	$Q\left(\sqrt{\frac{2N_s A E_p}{N_0}}\right)$
OOK	$0, a$	0	$Q\left(\sqrt{\frac{a^2 N_s A E_p}{2N_0}}\right)$
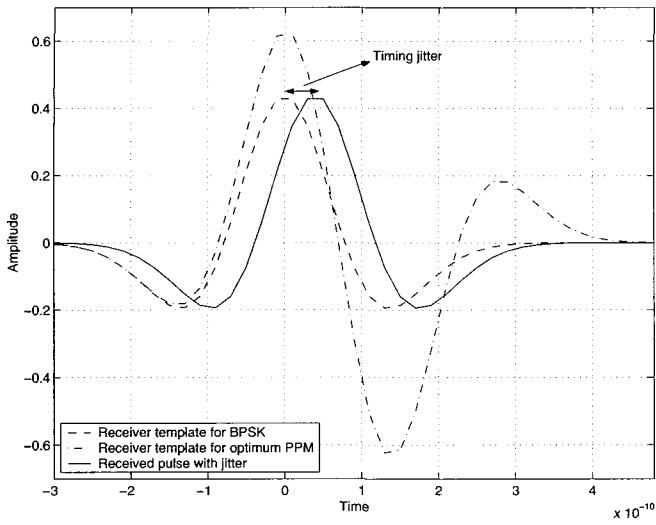
Fig. 1. Templates used at the correlator for BPSK and optimum PPM, and the received pulse with jitter ($\tau = 0.277$ ns).
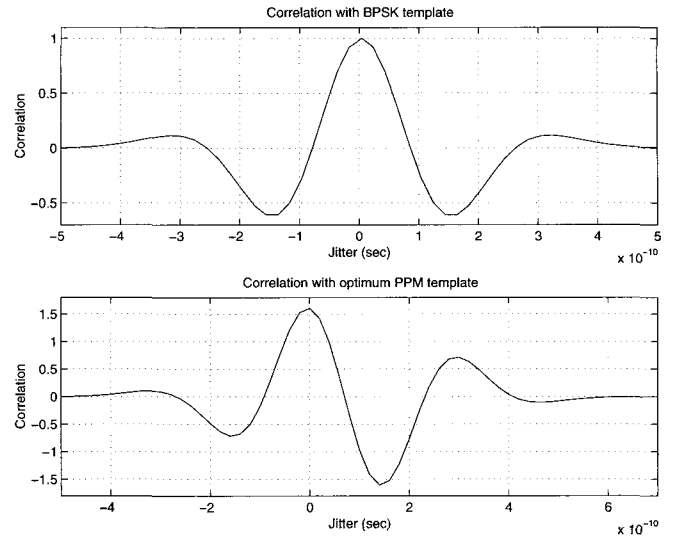
Fig. 2. Correlation functions of the received pulse with the templates used for BPSK and optimum PPM ($\tau = 0.277$ ns).

the SNRs after the correlator become zero when the timing jitter is around 80 ps, which determines a jitter budget for a typical UWB system employing the pulse shape in Fig. 1.

B. BER Performance Analysis

In order to evaluate the BER performances, it is required to analyze the correlator outputs of signal and noise separately. When PPM is used, correlation of the received pulse with the template, m_p, and the variance of the correlation of the noise with the template, σ_{corr}^2, can be respectively evaluated as follows [26]

$$m_p = \int_{-\infty}^{\infty} \omega_{rx}(t)v(t)dt,$$
$$= E_p[1 - R(\delta)] , \tag{11}$$

$$\sigma_{corr}^2 = E\left[\left(\int_{-\infty}^{\infty} \tilde{n}(t)v(t)dt\right)^2\right]$$
$$= \int_{-\infty}^{\infty}\int_{-\infty}^{\infty} v(t_1)v(t_2)E\left[\tilde{n}(t_1)\tilde{n}(t_2)\right]dt_1 dt_2$$
$$= N_0 E_p[1 - R(\delta)] . \tag{12}$$

The SNR after the correlator considering the pulse amplitude and the processing gain is calculated as

$$\text{SNR} = \frac{(N_s\sqrt{A}m_p)^2}{N_s\sigma_{corr}^2} . \tag{13}$$

Using (11) and (12) in (13),

$$\text{SNR} = \frac{N_s A E_p}{N_0}(1 - R(\delta)) . \tag{14}$$

Following a similar approach for other modulation schemes and using the standard techniques [17], [27], [28], BER performances for the four binary modulation schemes can be derived as shown in Table 1.

III. EFFECT OF TIMING JITTER ON BER PERFORMANCES

When there is timing jitter in the UWB signals, a deviation from its ideal timing position is observed in the received signal. This degrades the performance since jitter decreases m_p, the correlation of the received pulse with the receiver template. This section will cover the theoretical performance evaluation

Table 2. BER performances of UWB modulation schemes in AWGN channel and in the presence of timing jitter.

Modulation	BER
Orthogonal PPM	$Q\left(\sqrt{\frac{N_s AE_p}{N_0} R^2(\epsilon_j)}\right)$
Optimum PPM	$Q\left(\sqrt{\frac{N_s AE_p}{N_0} \frac{[R(\epsilon_j)-R(\delta_{opt}-\epsilon_j)]^2}{1-R(\delta_{opt})}}\right)$
BPSK	$Q\left(\sqrt{\frac{2N_s AE_p}{N_0} R^2(\epsilon_j)}\right)$
OOK	$\frac{1}{2}\left[Q\left(\sqrt{\frac{N_s AE_p}{N_0}}\right) + Q\left(\sqrt{\frac{N_s AE_p}{N_0}[2R(\epsilon_j)-1]^2}\right)\right]$

of different modulation schemes in the presence of timing jitter assuming that PDF of timing jitter is known. Uniform timing jitter is assumed throughout the section for simulation purposes[2], and the next section compares the performances for different distributions that have the same variance. BER performances in AWGN, single-tap Rayleigh fading, and dispersive channels are derived initially for a fixed value of the timing jitter, and averaged over the PDF of timing jitter to find the expected performance. Obtained theoretical findings are then verified by simulation results.

A. BER Performances in Static Channel

For a fixed value of the timing jitter, there is ϵ_j amount of timing difference between the actual and the ideal positions of the receiver template. Correlation values with the signal and the noise for PPM with a fixed value of timing jitter are calculated as

$$m_p = \int_{-\infty}^{\infty} \omega_{rx}(t + \epsilon_j)v(t)dt,$$
$$= E_p[R(\epsilon_j) - R(\delta - \epsilon_j)] , \qquad (15)$$

$$\sigma_{corr}^2 = E\left[\left(\int_{-\infty}^{\infty} \tilde{n}(t + \epsilon_j)v(t)dt\right)^2\right]$$
$$= \int_{-\infty}^{\infty}\int_{-\infty}^{\infty} v(t_1)v(t_2).$$
$$E[\tilde{n}(t_1 + \epsilon_j)\tilde{n}(t_2 + \epsilon_j)]\, dt_1 dt_2$$
$$= N_0 E_p[1 - R(\delta)] . \qquad (16)$$

Plugging (15) and (16) in (13), SNR for PPM for a fixed value of timing jitter is evaluated as follows

$$\text{SNR} = \frac{N_s AE_p}{N_0}\left[\frac{(R(\epsilon_j) - R(\delta - \epsilon_j))^2}{1 - R(\delta)}\right] . \qquad (17)$$

Note that in order to multiply the SNR with the processing gain N_s. it is assumed that all N_s pulses are subject to same amount of timing jitter. For orthogonal PPM, $R(\delta)$ becomes zero and the above equation reduces to

$$\text{SNR} = \frac{N_s AE_p}{N_0} R^2(\epsilon_j) . \qquad (18)$$

[2]Recall that although random jitter is assumed to be Gaussian, the total jitter, which is the sum of the random jitter and the deterministic jitter, can have different distributions.

For BPSK, using ω_{rec} as the receiver template and proceeding with a similar analysis yields

$$\text{SNR} = \frac{2N_s AE_p}{N_0} R^2(\epsilon_j) . \qquad (19)$$

Note that the effect of timing jitter on the system performance is the attenuation of the SNR with the corresponding correlation terms that depend on the employed pulse shape and modulation scheme.

For OOK modulation, reception of *zeros* are not affected by timing jitter since no pulse is sent for the transmission of *zeros*. Reception of *ones* will be degraded severely due to employed detection algorithm that compares the correlator output with a certain threshold. The resulting BER equation can be evaluated to be the sum of the *false alarm rate* and the *missed detection rate* using standard tools, which is shown in Table 2 together with performances of other modulation schemes. The value of a in Table 1 is taken as $\sqrt{2}$ to make the average transmitted energy of OOK identical with the other modulation schemes. Equations for BPSK and orthogonal PPM imply that SNRs in both schemes decrease in equal proportions, conserving the 3 dB power efficiency of the former scheme to the latter irrespective of the timing jitter.

Knowing the PDF of timing jitter, the calculated BER expressions can be integrated over all possible jitter values to evaluate the average performance. Assuming that timing jitter is uniformly distributed between $(-\epsilon_0, \epsilon_0)$ the BER performance can be evaluated as follows

$$P_{avg}(\Gamma, \epsilon_0) = \int_{-\epsilon_0}^{\epsilon_0} P_b(\Gamma, \epsilon_j)p(\epsilon_j)d\epsilon_j , \qquad (20)$$

where Γ denotes the SNR of the received signal, $P_{avg}(\Gamma)$ denotes the average BER corresponding to a certain jitter distribution at a certain SNR, $P_b(\Gamma, \epsilon_j)$ denotes the BER at a certain SNR and a fixed value of timing jitter as given in Table 2, and $p(\epsilon_j)$ is the probability density function of jitter, which is for uniform distribution given by

$$p(\epsilon_j) = \frac{1}{2\epsilon_0} . \qquad (21)$$

The integral in (20) can be evaluated semi-analytically to average the BER performance over all possible jitter values. Theoretical and simulation results for BPSK in AWGN channel are depicted in Fig. 3 for a fixed value of timing jitter and in Fig. 4
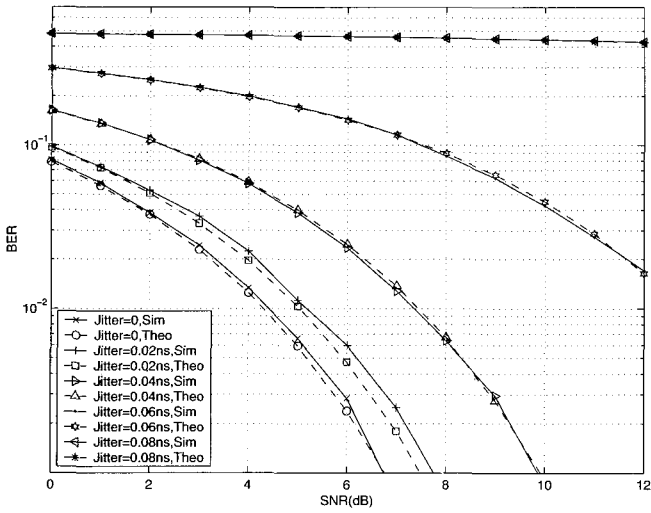
Fig. 3. BER performance of BPSK with constant jitter in AWGN channel ($T_c = T_h = 0.8$ ns, $N_s = 1$).

Fig. 5. Effect of the fixed value of timing jitter on the BER performances of different modulation schemes (SNR = 5 dB, $T_c = T_h = 0.8$ ns, N_s = 1).
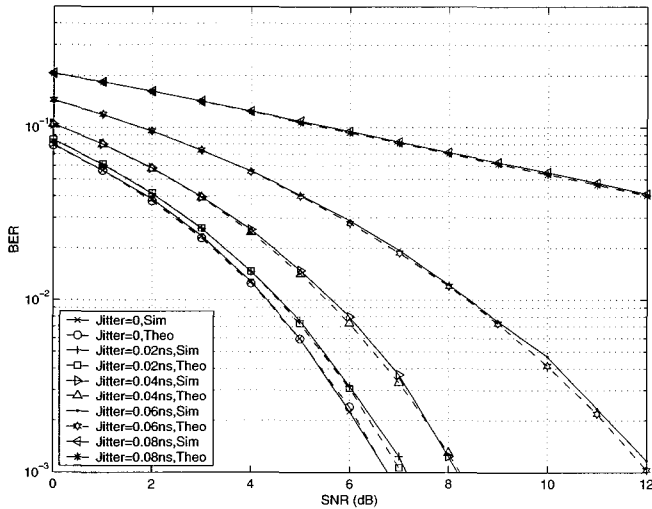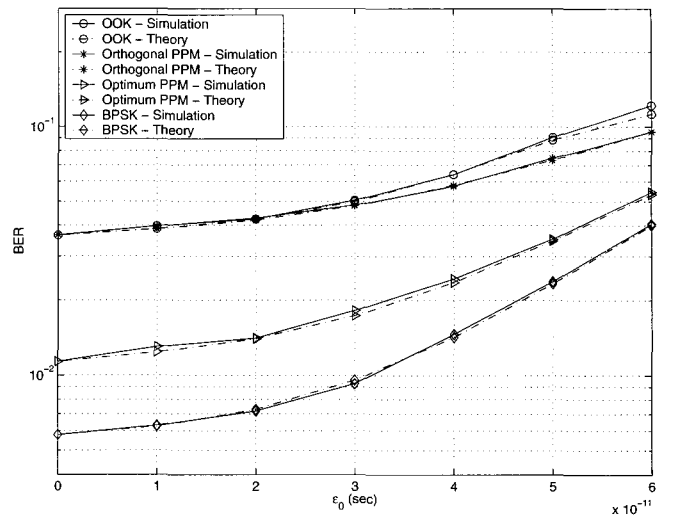

Fig. 4. BER performance of BPSK with uniform distributed jitter in AWGN channel ($T_c = T_h = 0.8$ ns, $N_s = 1$).

for jitter uniformly distributed between $\pm\epsilon_0$. Note that when the fixed value of jitter is 80 ps, accuracy of the detection is close to 50% since the SNR after the correlator output becomes very close to zero. Fig. 5 compares the performances of the four modulation schemes when jitter is uniformly distributed between $\pm\epsilon_0$, where it is seen that the gap between OOK and orthogonal PPM increases for larger values of timing jitter.

B. BER Performances in One-Tap Rayleigh Fading Channel

In one-tap Rayleigh fading channels, the received signal has a complex amplitude γ_l that has a Rayleigh distribution. In such environments, the probability of error is found by integrating the BER over all possible instantaneous SNR values [27]

$$P_{rayl}(\Gamma) = \int_0^\infty P_b(\Gamma, \gamma) p(\gamma) dA, \tag{22}$$

where γ is the instantaneous SNR of the received signal given by $\gamma_l^2 \frac{N_s A E_p}{N_0}$, Γ is the average SNR, $P_{rayl}(\Gamma)$ is the bit error

probability at a certain average SNR, and $p(\gamma)$ is the PDF of the instantaneous SNR values characterized by a chi-square distribution with two degrees of freedom which can be written as

$$p(\gamma) = \frac{1}{\Gamma} \exp\left(-\frac{\gamma}{\Gamma}\right) . \tag{23}$$

Plugging the error probabilities for different modulation schemes from Table 1 in (22), the closed form solution for the BER in Rayleigh fading channel is evaluated as

$$P_{rayl}(\Gamma) = \frac{1}{2}\left(1 - \sqrt{\frac{\Gamma'}{2 + \Gamma'}}\right), \tag{24}$$

where $\Gamma' = \Gamma$ for orthogonal PPM, $\Gamma' = 2\Gamma$ for BPSK, and $\Gamma' = \Gamma(1 - R(\delta))$ for optimum PPM. For a fixed value of timing jitter, the SNR values will be multiplied with the corresponding autocorrelation values as summarized in Table 3.

For uniformly distributed timing jitter, BER in Rayleigh fading channel can be evaluated by a numerical integration of expressions in Table 3 over all possible jitter values as

$$P_{avg}(\Gamma, \epsilon_0) = \int_{-\epsilon_0}^{\epsilon_0} P_{rayl}(\Gamma, \epsilon_j) p(\epsilon_j) d\epsilon_j . \tag{25}$$

Performance results for BPSK in Rayleigh fading channel for a fixed value of jitter and for uniformly distributed jitter are depicted in Figs. 6 and 7. Similar comments as in AWGN channel can be repeated, together with an observation of overall performance degradation for all jitter scenarios due to fading.

C. BER Performances in Dispersive Channel

Due to reflection, diffraction, and scattering effects, the transmitted signal arrives at the receiver through multiple paths with different delays. The received signal from an N-tap channel can be written as follows

$$r_{mp}(t) = \sum_{l=1}^{N} \gamma_l s^{(k)}(t - \tau_l) + n(t) , \tag{26}$$

Table 3. BER performances of UWB modulation schemes in Rayleigh fading channel and in the presence of timing jitter.

Modulation	BER
Orthogonal PPM	$\frac{1}{2}\left(1 - \sqrt{\frac{\Gamma R^2(\epsilon_j)}{2+\Gamma R^2(\epsilon j)}}\right)$
Optimum PPM	$\frac{1}{2}\left(1 - \sqrt{\frac{\Gamma R_{opt}}{2+\Gamma R_{opt}}}\right)$, $R_{opt} = \frac{[R(\epsilon_j)-R(\delta_{opt}-\epsilon_j)]^2}{1-R(\delta_{opt})}$
BPSK	$\frac{1}{2}\left(1 - \sqrt{\frac{\Gamma R^2(\epsilon_j)}{1+\Gamma R^2(\epsilon j)}}\right)$
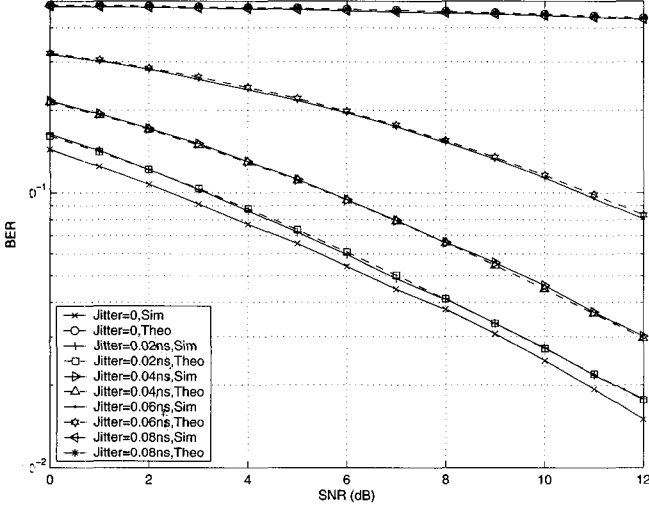
Fig. 6. BER performance of BPSK with constant jitter in Rayleigh fading channel ($T_c = T_h = 0.8$ ns, $N_s = 1$).
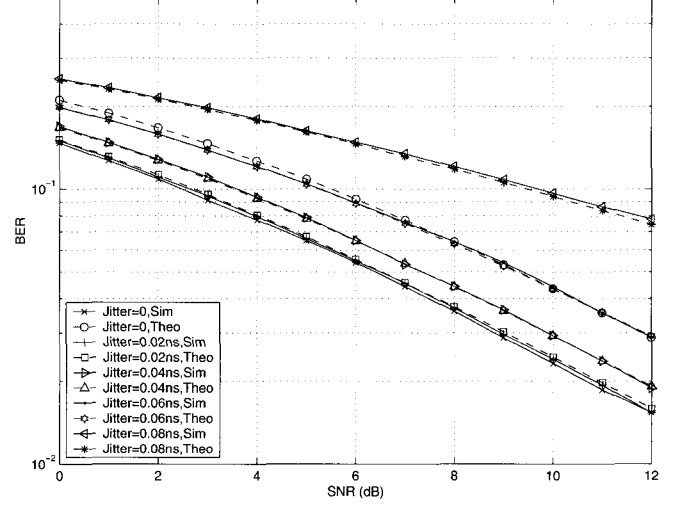
Fig. 7. BER performance of BPSK with uniform distributed jitter in Rayleigh fading channel ($T_c = T_h = 0.8$ ns, $N_s = 1$).

where γ_l is the tap attenuation for the lth tap arriving at time τ_l and $s^{(k)}(t)$ is the transmitted signal from (1).

By using Rake receivers, it is possible to collect the energy at the delayed taps. *All-Rake, selective Rake,* or *partial Rake* receivers are all feasible approaches to collect all, strongest, or first arriving resolvable multipath components respectively [29]. Optimal combining of the multipath components is achieved by maximal ratio combining (MRC) in white noise, where the finger weights are designed based on the channel tap weights to maximize the output SNR. A reduced complexity combining technique that does not require the estimates of the fading amplitudes is equal gain combining (EGC), where all the multipath components are weighted equally.

The PDF of the instantaneous SNR when using MRC is given by [27]

$$p(\gamma) = \sum_{k=1}^{N} \frac{\pi_k}{\Gamma_k} e^{-\frac{\gamma}{\Gamma_k}}, \qquad (27)$$

$$\pi_k = \prod_{i=1, i\neq k}^{N} \frac{\Gamma_k}{\Gamma_k - \Gamma_i}, \qquad (28)$$

where Γ_k is the average SNR for the kth tap. Knowing the PDF of the SNR, BER equation for AWGN can be conditioned on the instantaneous SNR and the average BER performance can be evaluated through integration over all possible SNR values. For example for BPSK, average performance using MRC in the

presence of fixed timing jitter is given by

$$P_{mpath}(\Gamma, \epsilon_j) = \int_0^\infty p(\gamma)\frac{1}{2}\mathrm{erfc}\left(\sqrt{\gamma R^2(\epsilon_j)}\right) d\gamma, \qquad (29)$$

where it is assumed that all multipath taps are subject to same amount of timing jitter. This formulation can again be integrated over the PDF of timing jitter to find the average performance in the presence of uniformly distributed jitter

$$P_{avg}(\Gamma, \epsilon_0) = \int_{-\epsilon_0}^{\epsilon_0} P_{mpath}(\Gamma, \epsilon_j)p(\epsilon_j)d\epsilon_j. \qquad (30)$$

Performance results for BPSK using MRC Rake receivers for a fixed value of jitter and for uniformly distributed jitter are shown in Figs. 8 and 9. A four tap Rayleigh fading channel profile with exponentially distributed average tap weights is assumed, and a Rake receiver with four fingers is employed, which assumes a perfect knowledge of the channel. Notice how the performance is improved compared to one-tap Rayleigh fading channel when using maximal ratio diversity combining. Different channel models (such as the channel measurements presented in [30], or IEEE 802.15 channel model [31]) can be easily integrated to the formulation outlined above, since the performance is a function of average tap weights.
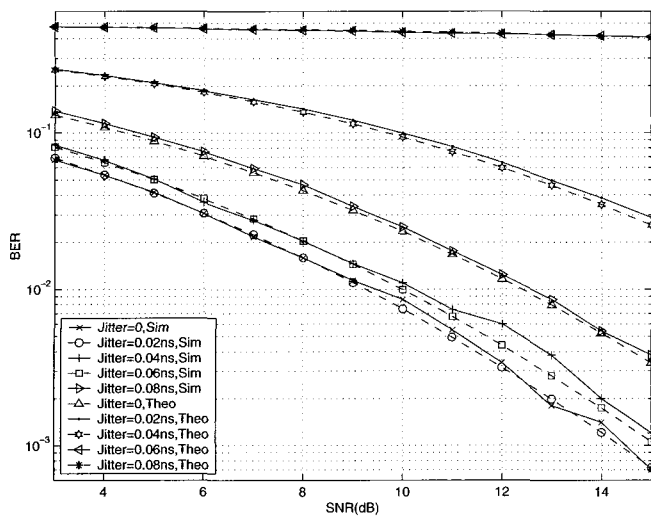
Fig. 8. BER performance of BPSK with constant jitter in 4-tap multipath fading channel (exponential power delay profile) using MRC Rake receiver ($T_c = T_h = 0.8$ ns, $N_s = 1$).

Fig. 10. Probability densities of finger estimation errors ($T_c = T_h = 0.8$ ns).
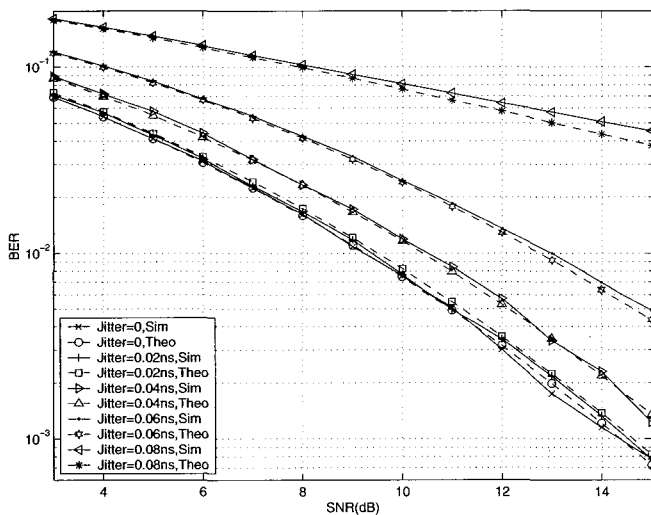

Fig. 9. BER performance of BPSK with uniform distributed jitter in 4-tap multipath fading channel (exponential power delay profile) using MRC Rake receiver ($T_c = T_h = 0.8$ ns, $N_s = 1$).

IV. EFFECT OF TIMING JITTER DISTRIBUTION ON SYSTEM PERFORMANCE

In the previous section, it is assumed that timing jitter is uniformly distributed. Sources of timing jitter can be numerous, and therefore jitter can have different distributions. Sometimes, the timing jitter can be characterized by its range and RMS value only, where an upper bound for system performance is helpful to evaluate the worst case performance. In this section, first, jitter due to finger estimation error is introduced and its PDF is obtained using simulations. Later, effect of jitter PDF on system performance is analyzed and a worst case distribution given the variance and the range of the timing jitter is presented.
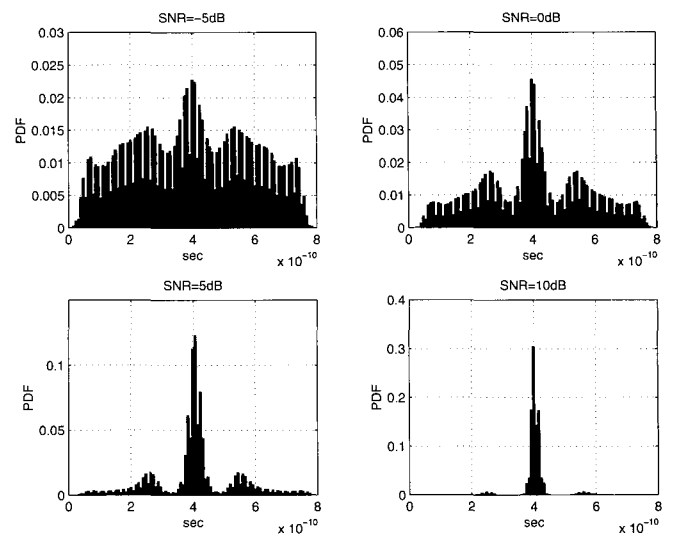
A. Jitter due to Finger Estimation

Due to UWB delay resolution, Rake receivers have been widely proposed in order to exploit time diversity in multipath channels. Rake receiver requires the knowledge of the path delays to be able to lock on each correlator (finger) and coherently add the energy, increasing SNR. As explained in [32], finding the path locations is not an easy task due to pulse shaping. For each arriving path to the receiver, the pulse shape observed after correlation contains many components with non-zero energy. Finger estimation maximizes this correlation function in order to pick up the component with more energy. In the presence of noise, autocorrelation function may be maximized at times other than the actual position of the finger, which yields a finger estimation error. The timing jitter due to such an impairment may be on the order of the pulse width T_c and depends on the SNR value.

Jitter due to transceiver impairments are commonly modeled as Gaussian or uniform, but these models are no longer valid for finger estimation error. In order to find the appropriate model, finger estimation error is simulated for different SNR scenarios to obtain a histogram of resulting timing jitter. PDFs for different SNR values in Fig. 10 show that when SNR is low, the PDF is similar to the autocorrelation function of the first derivative of the monopulse, and finger locations are estimated between zero and T_c. For larger SNR, the PDF converges to an impulse function located at the actual position of the finger.

B. Effect of Jitter PDF on the BER Performance

It is shown in the previous section that in order to estimate the effect of timing jitter on the BER performance, PDF of timing jitter has to be known. Note that obtaining PDF would be difficult in many cases, instead statistics like RMS value and range (minimum and maximum jitter values) can be measured [6]. Given the variance, σ_ϵ^2, and the range, r_ϵ, of timing jitter, a worst case distribution (WCD) that will cause the largest degradation
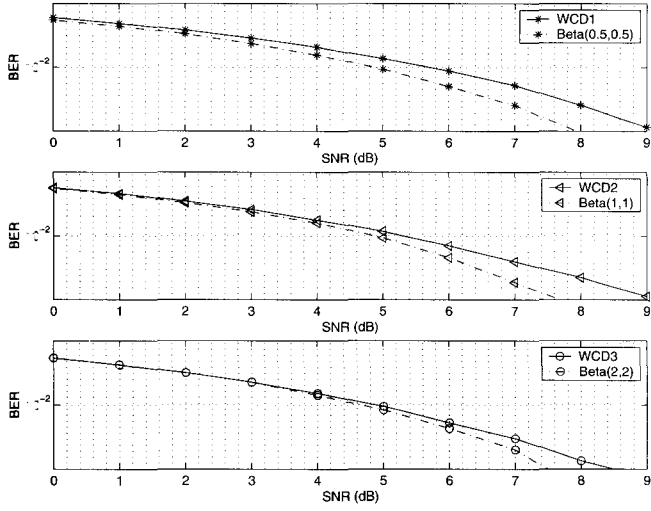
Fig. 11. BER performance of BPSK for different jitter distributions in AWGN channel ($T_c = T_h = 0.8$ ns, $N_s = 1$).
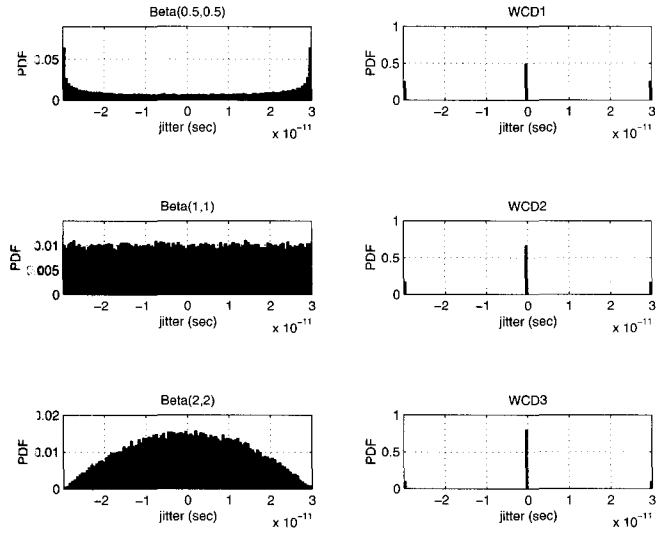

Fig. 12. Histograms for the timing jitter used in the simulations and the corresponding worst case distributions that have the same variance and the range.

in system performance is given as [6], [7]

$$p(\epsilon) = \frac{\sigma_\epsilon^2}{2r_\epsilon^2} [\delta_D(\epsilon_j - r_\epsilon) + \delta_D(\epsilon_j + r_\epsilon)] + \left(1 - \frac{\sigma_\epsilon^2}{r_\epsilon^2}\right) \delta_D(\epsilon_j),$$
(31)

where δ_D denotes the Dirac delta function. Given the range and the variance of the timing jitter, this PDF yields an upper bound for the system performance irrespective of the jitter distribution that has the same range and variance. Note that one can easily change the variance of the WCD without modifying its range.

In order to compare the BER performances using different jitter distributions, random timing jitter are constructed using the Beta probability distribution with different parameters, given
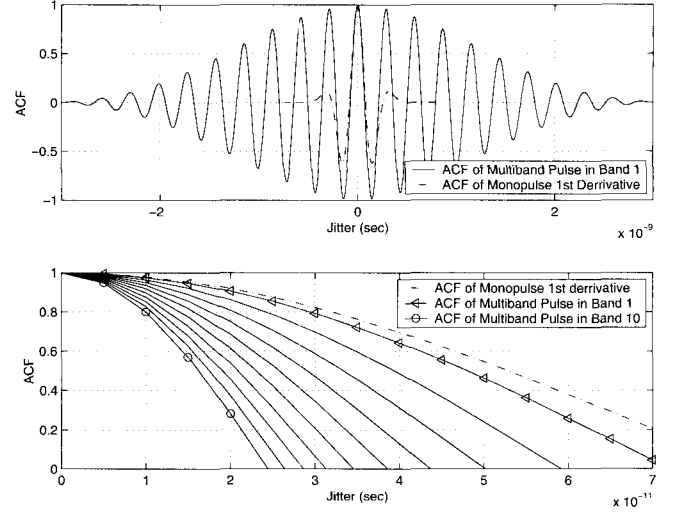

Fig. 13. Comparison of autocorrelation functions of derivative of monocycle vs. pulse used in band 1 of multiband scheme, and comparison of the autocorrelations of the pulses used in all bands.

by [33]

$$p(\epsilon_j, p, q) = \frac{\epsilon_j^{p-1}(1 - \epsilon_j)^{q-1}}{B(p, q)}, 0 \le \epsilon_j \le 1,$$
(32)

$$B(p, q) = \int_0^1 t^{p-1}(1 - t)^{q-1} dt.$$
(33)

The PDFs for the three different Beta distributions characterized by the parameters $(p, q) = (2, 2)$ to represent a bounded Gaussian-like distribution, $(p, q) = (1, 1)$ which corresponds to the uniform distribution, and $(p, q) = (0.5, 0.5)$ that has largest probability at the edges of the distribution are depicted in Fig. 12. All the three distributions are scaled so that the range of the timing jitter is ± 30 ps, which can be used as a typical margin for UWB systems [16]. For each Beta distribution, a worst case distribution with the same variance and range is evaluated, and obtained jitter samples are used in computer simulations. Performance results in Fig. 11 for BPSK show that WCD indeed yields an upper bound for another distribution that has the same variance and range. Beta distribution with $(p, q) = (0.5, 0.5)$ yields the worst performance compared to other Beta distributions, since it resembles to the WCD with the peaks at the edges of the distribution. Bounded Gaussian-like distribution has the best performance, because as mentioned in the previous section, performance degradation for small jitter values is negligible. Tightness of the worst case bound increases from the former to the latter.

V. EFFECT OF TIMING JITTER ON THE PERFORMANCE OF SYSTEMS WITH DIFFERENT PULSE SHAPES

As shown in Section III (Tables 2 and 3), autocorrelation function of the employed pulse shape for a certain jitter value is a direct measure of the system performance. If the autocorrelation function decays faster, UWB performance will be more

affected from timing jitter. In this section, effect of timing jitter on the performances of multiband [34] and modified Hermite polynomial based [35] UWB schemes are investigated.

Multiband UWB scheme is achieved by dividing UWB spectrum into a number of frequency bands by using a different pulse shape at each band. In order to adjust the central frequency of each band, pulses used at higher order bands have larger frequencies. This approach has a number of advantages, such as mitigating interference by not transmitting at the band(s) that are occupied by other technologies, or adjusting the data rate by using desired number of bands. In spite of these advantages, multiband scheme is more susceptible against timing jitter for higher order bands since the autocorrelation function of pulses used at these bands decay faster. In order to see the effect of timing jitter, a sample multiband scheme is constructed by dividing the $3.1 - 10.6$ GHz band into ten bands of 750 MHz each. The autocorrelation functions of the pulse used in band-1 ($3.1 - 3.85$ GHz) of multiband scheme and the pulse in (3) which is used in standard UWB scheme are compared in Fig. 13. It is seen that since the central frequencies of both systems are close, similar degradation will be observed in the performances. Fig. 13 also compares the autocorrelation functions of the pulses used in different bands of the multiband scheme with respect to the fixed timing jitter value that ranges from 0 to 70 ps. It is observed that degradation due to timing jitter when using multiband scheme will be worse for higher order bands.

A similar analysis can be repeated for UWB schemes that employ modified Hermite polynomial based pulses [35]. Using these polynomials, it is possible to construct a new pulse that is orthogonal to the previous pulses by using certain transformations. Such higher order pulses have larger number of zero crossings and their autocorrelation functions decay faster, implying less robustness against timing jitter [25].

VI. CONCLUSION

In this paper, a framework that enables evaluation of the performances of different UWB modulation schemes in the presence of timing jitter is presented. It is observed that the performances of BPSK and PPM are degraded similarly, while OOK yields biased decisions towards zero. The PDF of timing jitter due to finger estimation error is presented using simulations. It is shown that the PDF depends on the employed pulse shape and the SNR. A worst case distribution that minimizes the system performance is also given and compared with other distributions that have the same variance and range. It is shown that for a given jitter range and variance, the worst case distribution provides an upper bound regardless of the jitter distribution. Dependency of the BER performance on the employed pulse shape is analyzed, and it is concluded that if the autocorrelation function of the employed pulse decays faster, the UWB system is more susceptible against timing jitter. Finally, the effect of timing jitter on the recently proposed multiband scheme is evaluated, where the higher bands are observed to be more susceptible against timing jitter as the pulses corresponding to those bands have narrower main lobes. As a result, users have to use time-frequency hopping codes so that every user benefits/suffers equivalently from all the bands.

REFERENCES

[1]   P. R. Trischitta and E. L. Varma, *Jitter in Digital Transmission Systems*, 1st ed. Norwood, MA: Artech House Inc., 1989.
[2]   S. Haykin, *Communication Systems*, 3rd ed. New York: John Wiley and Sons, Inc., 1994, pp. 461–465.
[3]   C. Duff, "Jitter analysis techniques," Agilent Technologies, p. 1, 2002, available at http://www.agilent.com.
[4]   J. Sun, M. Li, and J. Wilstrup, "A demonstration of deterministic jitter (DJ) deconvolution," in *Proc. IEEE Instrumentation Measurement Technol. Conf. (IMTC)*, vol. 1, Anchorage, AK, May 2002, pp. 293–298.
[5]   Maxim High-Frequency/Fiber Communications Group, "Jitter in digital communication systems, part 1," Application note, HFAN-4.0.3, pp. 2–6, Sept. 2001, available at http://pdfserv.maxim-ic.com/arpdf/AppNotes/5hfan403.pdf.
[6]   K. Schumacher and J. J. O'reily, "Distribution free bound on the performance of optical communication systems in the presence of jitter," *IEE Proceedings*, vol. 136J, no. 2, pp. 129–136, Apr. 1989.
[7]   Z. Nikolic, M. Stefanovic, and N. Stojanovic, "Upper bound of error probability in the presence of intersymbol interference and jitter," *IEE Electron. Lett.*, vol. 30, no. 5, pp. 389–390, Mar. 1994.
[8]   L. Tomba and W. A. Krzymien, "Performance enhancement of multicarrier CDMA systems impaired by chip timing jitter," in *Proc. IEEE Int. Symp. Spread Spectrum Techniques Appl.*, vol. 1, Sept. 1996, pp. 22–25.
[9]   B. Kaushik, R. Ganesh, and R. Sadhu, "Modeling delay jitter distribution in voice over IP," Jan. 2003, unpublished, available at http://arxiv.org/pdf/cs.PF/0301005.
[10] S. Shenghe, G. Shize, and L. Chunming, "An adaptive deconvolution method for eleminating the effect of the time jitter," in *Proc. IEEE Instrumentation Measurement Technol. Conf. (IMTC)*, vol. 3, Hamamatsu, Japan, May 1994, pp. 1140–1142.
[11] M. P. Li et al., "A new method for jitter decomposition through its distribution tail fitting," in *Proc. IEEE Int. Test Conf. (ITC)*, Atlantic City, NJ, Sept. 1999, pp. 788–794.
[12] C. Mailhes and B. Lacaze, "Jitter effects in a multipath environment," in *Proc. IEEE Int. Conf. Acoustics Speech Sig. Processing (ICASSP)*, vol. 6, Salt Lake City, UT, May 2001, pp. 3905–3908.
[13] M. Shimanouchi, "An approach to consistent jitter modelling for various jitter aspects and measurement methods," in *Proc. IEEE Int. Test Conf. (ITC)*, Baltimore, MD, Nov. 2001, pp. 848–857.
[14] Y. Takasaki, *Digital Transmission Design and Jitter Analysis*, 1st ed. Norwood, MA: Artech House Inc., 1991.
[15] D. Kelly et al., "PulsON second generation timing chip: Enabling UWB through precise timing," in *Proc. IEEE Conf. UWB Syst. Technol.*, Maryland, USA, 2002, pp. 117–121.
[16] W. M. Lovelace and J. K. Townsend, "The effects of timing jitter and tracking on the performance of impulse radio," *IEEE J. Select. Areas Commun.*, vol. 20, no. 9, pp. 1646–1651, Dec. 2002.
[17] X. Huang and Y. Li, "Performances of impulse train modulated ultrawideband systems," in *Proc. IEEE Int. Conf. Commun. (ICC)*, vol. 2, New York City, NY, 2002, pp. 758–762.
[18] L. Ge, G. Yue, and S. Affes, "On the BER performance of pulse-position-modulation UWB radio in multipath channels," in *Proc. IEEE Conf. UWB Syst. Technol.*, vol. 3, Maryland, USA, May 2002, pp. 231–234.
[19] G. Durisi and S. Benedetto, "Performance evaluation and comparison of different modulation schemes for UWB multiaccess systems," in *Proc. IEEE Int. Conf. Commun. (ICC)*, vol. 3, Anchorage, AK, May 2003, pp. 2187–2191.
[20] M. Hamalainen et al., "On the performance comparison of different UWB data modulation schemes in AWGN channel in the presence of jamming," in *Proc. IEEE Radio and Wireless Conf. (RAWCON)*, Boston, MA, Aug. 2002, pp. 83–86.
[21] M. Z. Win, "A unified spectral analysis of generalized time-hopping spread-spectrum signals in the presence of timing jitter," *IEEE J. Select. Areas Commun.*, vol. 20, no. 9, pp. 1664–1676, Dec. 2002.
[22] ——, "Spectral density of random time-hopping spread-spectrum UWB signals with uniform timing jitter," in *Proc. IEEE Mil. Commun. Conf. MILCOM*, vol. 2, Atlantic City, NJ, Nov. 1999, pp. 1196–1200.
[23] ——, "Spectral density of random UWB signals," *IEEE Commun. Lett.*, vol. 6, no. 12, pp. 526–528, Dec. 2002.
[24] Y. Shin and J. Ahn, "Effect of timing jitter in an ultra wideband impulse radio system," in *Proc. IEEE Int. Symp. on Intelligent Signal Processing and Commun. Syst. (ISPACS)*, Hawaii, Nov. 2000, pp. 502–505.

[25] L. B. Michael, M. Ghavami, and R. Kohno, "Effect of timing jitter on Hermite function based orthogonal pulses for ultra wideband communication," in *Proc. 4th Int. Symp. Wireless Personal Multimedia Commun.*, Aalborg, Denmark, Sept. 2001, pp. 441–444.

[26] M. Win and R. A. Scholtz, "Ultra-wide bandwidth time-hopping spread-spectrum impulse radio for wireless multiple-access communications," *IEEE Trans. Commun.*, vol. 48, no. 4, pp. 679–689, Apr. 2000.

[27] J. G. Proakis, *Digital Communications*, 3rd ed. New York: McGraw Hill, Inc., 1995, pp. 801–802.

[28] I. Guvenc and H. Arslan, "On the modulation options for UWB systems," in *Proc. IEEE Mil. Commun. Conf. MILCOM*, Boston, MA, Oct. 2003.

[29] D. Cassioli *et al.*, "Performance of low-complexity RAKE reception in a realistic UWB channel," in *Proc. IEEE Int. Conf. Commun. (ICC)*, vol. 2, New York, Apr. 2002, pp. 763–767.

[30] M. Z. Win and R. A. Scholtz, "Characterization of ultra-wide bandwidth wireless indoor channels: A communication theoretic view," *IEEE J. Select. Areas Commun.*, vol. 20, no. 9, pp. 1613–1627, Dec. 2002.

[31] J. Foerster, "IEEE P802.15 working group for wireless personal area networks (WPANs), channel modeling sub-committee report - final," Mar. 2003, available at http://www.ieee802.org/15/pub/2003/Mar03/.

[32] F. E. Aranda, N. Brown, and H. Arslan, "Rake receiver finger assignment for ultra-wideband radio," in *IEEE Workshop Sig. Proc. Adv. Wireless Commun. (SPAWC)*, Rome, Italy, June 2003.

[33] "NIST/SEMATECH e-Handbook of statistical methods," June 2003, available at http://www.itl.nist.gov/div898/handbook/.

[34] G. R. Aiello and G. D. Rogerson, "Ultra-wideband wireless systems," *IEEE Microwave*, vol. 4, no. 2, pp. 36–47, June 2003.

[35] M. Ghavami, L. B. Michael, and R. Kohno, "Hermite function based orthogonal pulses for for ultra wideband communication," in *Proc. 4th Int. Symp. Wireless Personal Multimedia Commun.*, Aalborg, Denmark, Sept. 2001. pp. 437–440.

Hüseyin Arslan has received his PhD. degree in 1998 from Southern Methodist University (SMU), Dallas, Tx. From January 1998 to August 2002, he was with the research group of Ericsson Inc. at RTP, NC. Since August 2002, he has been with the Electrical Engineering Dept. of University of South Florida. In Ericsson, he was involved with several project related to 2G and 3G wireless cellular communication systems. His research interests are related to advanced signal processing techniques at the physical layer, with cross-layer design for networking adaptivity and Quality of Service (QoS) control. More specifically, he is interested in signal processing techniques for wireless communication systems including modulation and coding, interference cancellation and multi-user signal detection, channel estimation and tracking, equalization, soft information generation, adaptive receiver, and transmission technologies, etc. He has authored and co-authored 2 book chapters, and published more than 35 technical papers on various IEEE journals and conferences. He also has more than 15 patents; some are already issued and mostly pending. He has served as session chair, session organizer, and as technical program committee member in several IEEE conferences. He is member of editorial board for Wireless Communication and Mobile Computing journal, and he has served as co-chair for 3 symposiums in IEEE VTC'03.
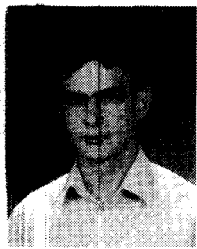
İsmail Güvenç was born in Istanbul, Turkey, on May 28, 1979. He has received his B. S. degree from Electrical Engineering, Bilkent University, Ankara, Turkey in 2001, and M.S. degree from Electrical and Computer Engineering, University of New Mexico, Albuquerque, NM in 2003, with a thesis on indoor geolocation systems. He is currently working toward his Ph.D. degree in Electrical Engineering Department of University of South Florida, Tampa, FL. His research interests are in signal processing for ultrawideband communications and networks, more specifically in multiuser detection, multiple access code design, synchronization, and performance analysis.